Report series ISSN 0284 – 2769 of
THE SVEDBERG LABORATORY and
DEPARTMENT OF RADIATION SCIENCES
UPPSALA UNIVERSITY
Box 533, S-751 21 Uppsala, Sweden
http://www.tsl.uu.se/

arXiv:nucl-th/9812004v1 1 Dec 1998

TSL/ISV-98-0201
December 1998

Structure in two-pion production in the $dd \to \alpha X$ reaction

Anders Gårdestig[1] and Göran Fäldt[2]
Division of Nuclear Physics, Uppsala University, Box 535,
S-751 21 Uppsala, Sweden

Colin Wilkin[3]
University College London, London WC1E 6BT, UK

Abstract: A model for the $dd \to \alpha\pi\pi$ reaction, based on two parallel $NN \to d\pi$ reactions, is extended to incorporate a complete set of input amplitudes. While low-energy cross sections are underestimated, the rich structure observed in the α-particle momentum distributions for $0.8 < T_d < 1.9$ GeV (the ABC effect) is extraordinarily well reproduced. In addition, a recent measurement of deuteron analyzing powers agrees quite well with our predictions, both in frequency and magnitude of the oscillations.

[1]grdstg@tsl.uu.se
[2]faldt@tsl.uu.se
[3]cw@hep.ucl.ac.uk

1 Introduction

On many occasions, interesting physics has been obtained from detailed studies of momentum distributions from nuclear reactions. Excitement once arose from the unexpected width of β-decay spectra, which led Pauli to postulate the existence of the neutrino. In most cases, however, the interest has focused on details of the distributions, such as an enhancement or a suppression at a certain missing mass, or skewness, or other irregularities. These deviations from phase space mark the discoveries of new particles and resonances, increased propensity for a particular partial wave, or some other peculiarity. Regardless of the problem at hand, further investigations often proved fruitful and well worth the effort. A particular interesting problem of this kind is the striking phenomenon observed in several experiments on the $pn \rightarrow dX$ [1, 2, 3], $pd \rightarrow {}^3\mathrm{He}X$ [4, 2, 5], and $dd \rightarrow \alpha X$ [6, 7] reactions. In all three cases there is a peak just above the two-pion threshold with a missing mass M_X $\approx$300–320 MeV/c^2. Since its position and width vary with kinematical conditions, it could not be a new particle or resonance. The only alternative is some sort of kinematical enhancement in double pion production. The experiments reveal that the effect only occurs in the isospin $I_X = 0$ channels of the two first reactions; the $dd \rightarrow \alpha X$ reaction leads to a pure $I_X = 0$ state, which is probably the reason for the more pronounced peaks in this case. In association with the peaks at low $\pi\pi$ mass there are also broad bumps at maximal missing masses. These are most clearly seen in the $pn \rightarrow dX$ and $dd \rightarrow \alpha X$ reactions, which could be due to more symmetric kinematics. These characteristics are collectively known as the ABC effect after the discoverers [4]. The suggestion of the original authors that the peaks are due to a large $\pi\pi$ s-wave scattering length was soon ruled out by separate experiments [8] and theoretical calculations [9]. In addition the central bump (unknown at the time) cannot be explained in this way, since it would mean that parallel and anti-parallel pions are simultaneously favored by the $\pi\pi$ interaction, which is very unlikely. The mass of the central bump is also changing monotonically with beam energy. It is thus impossible to explain the ABC enhancement in terms of some peculiarity of the $\pi\pi$ interaction and one has to include effects resulting from the presence of other particles in the reactions and consider the structure of the single pion production mechanism itself. In all three reactions there are indications that the ABC effect disappears at low beam energies [10, 11, 12, 13], suggesting that the subprocesses in any explanation should be strongly energy and angular dependent in order to reproduce the quite different dynamics observed in the different energy regions.

For the $pn \rightarrow dX$ reaction, on which theoretical investigations have mainly focused, the most promising approach is the $\Delta\Delta$-model [14]. Here two independent pion productions are achieved through the excitation of both incident nucleons into Δ-isobars via meson exchange, with the deuteron then being formed through a final state interaction of the recoil nucleons arising from the Δ decay. By using the energy and angular dependences of Δ-excitation and decay, the authors could

reproduce the shape quite well, but underestimate the cross section at larger angles [3]. A double-nucleon exchange model, also proposed in the seventies [15] and using separate diagrams for the three different peaks, showed a much poorer angular distribution [3] and the authors were incapable of obtaining an absolute normalization. In his survey of all ABC experiments and models, Barry [16] tried to improve the original $\Delta\Delta$-model and to extend it to $pd \to {}^3\mathrm{He}X$ but with little success; his model has, in particular, problems in reproducing the spectra away from the ABC peaks. Better results were achieved in a chiral bag model [17], taking into account 80 diagrams to fourth order in the πNN coupling constant, but this model still failed in the details. A model based on excitation of the $N^*(1440)$ (Roper) resonance has recently been proposed for the lower energies [18]. The calculations are in good agreement with data [10], but the contribution from $\Delta\Delta$ excitations is negligible. The situation at low energies is thus improving and might form a basis for a renewed investigation of the ABC effect in the $pn \to dX$ reaction.

Despite these efforts, there is as yet no completely satisfactory implementation of a model for the ABC enhancement in either the $pn \to dX$ or $pd \to {}^3\mathrm{He}X$ reactions. On the other hand, the $dd \to \alpha X$ reaction has not been subjected to any theoretical investigation because of its perceived complexity. In a preliminary study [19] we were able to reproduce very well the angular dependence measured at $T_d = 1.25$ GeV [6] using a version of a $\Delta\Delta$ model where independent single pion productions arise from two $NN \to d\pi$ reactions occurring in parallel. In this work, only the dominant $NN \to d\pi$ input amplitude was kept and we now lift this restriction by including a complete set of amplitudes. This makes it possible to reproduce all the major features observed in the $dd \to \alpha X$ reaction throughout the Δ region, including also the recent measurement of deuteron analyzing powers [7]. The main idea behind the model is explained in Sec. 2. The general description is then given a precise formulation in Sec. 3, to be followed by some remarks about the numerical calculations in Sec. 4. Our predictions are compared with data in Sec. 5 and conclusions and outlook are given in Sec. 6. Some formulae for the $NN \to d\pi$ reaction, in particular the relations between the partial wave and spin amplitudes, are collected in an appendix.

2 Model for $dd \to \alpha\pi\pi$

Our model for the $dd \to \alpha\pi\pi$ reaction is based on a simple, semi-classical picture and illustrated as a Feynman diagram in Fig. 1. The two-pion production in the dd collision is viewed as two free, parallel, and independent $NN \to d\pi$ reactions taking place between separate pairs of nucleons from the two deuterons. The α-particle is then formed by fusing the two final deuterons.

An intuitive motivation for this model can be obtained by looking at the possible configurations of final particles. If the deuteron and α-particle binding

energies are neglected, the local $NN \to d\pi$ cm frames obviously coincide with the overall cm (CM) so that the two deuterons have the same energy, though not necessarily the same directions. However, because of the strong p-wave dependence of the $NN \to d\pi$ reaction, the deuterons and pions are preferentially emitted at small angles to the beam direction. When deuterons are emitted parallel to each other, they are easily bound together into an α-particle. Due to the kinematics, the associated produced pions then have small relative momenta and hence small invariant mass. This corresponds to the situation at the ABC peaks. In the second case of anti-parallel deuterons, the pions go back-to-back, their invariant mass is maximal and this is the reason for the central bump. However, it then needs a lot of Fermi momentum in the initial deuterons and/or final α-particle in order to get the deuterons to stick together so that, despite the kinematical enhancement of this configuration, it is suppressed compared to the parallel case.

Both the ABC effect and the central bump are simultaneously explained in our model by the strong p-wave dominance in the $NN \to d\pi$ reaction, with the former being helped by favorable kinematics.

3 Formal description

The considerations of the previous section are immediately transformed into the Feynman diagram of Fig. 1, where the momenta of the particles are defined in the CM. In the following paragraphs the different parts of the corresponding matrix element are established using a description in terms of non-relativistic wave functions. The derivation of phase space formulae is also given.

3.1 Relativistic phase space

The phase space calculations for the $dd \to \alpha\pi^+\pi^-$ reaction are performed relativistically starting from the general expression [20]

$$\mathrm{d}\sigma = \frac{1}{|\mathbf{v}_{\mathrm{in}}|}\frac{1}{2E_1}\frac{1}{2E_2}|\mathcal{M}|^2\frac{\mathrm{d}^3k_1\mathrm{d}^3k_2\mathrm{d}^3k_\alpha}{(2\pi)^9 2\omega_1 2\omega_2 2\omega_\alpha}(2\pi)^4\,\delta^4(p_1+p_2-k_1-k_2-k_\alpha)\,, \quad (3.1)$$

where $E_i, \mathbf{p}_i$ and $\omega_j, \mathbf{k}_j$ are the energies and momenta of the initial and final particles, respectively. The α-particle is detected in the laboratory frame and thus $|\mathbf{v}_{\mathrm{in}}| = p/E$ and $\mathrm{d}^3k_\alpha/\omega_\alpha = [k_\alpha^2\,\mathrm{d}\Omega_\alpha \mathrm{d}k_\alpha/\omega_\alpha]_{\mathrm{lab}}$, so that

$$\left(\frac{\mathrm{d}^2\sigma}{\mathrm{d}\Omega_\alpha \mathrm{d}k_\alpha}\right)_{\mathrm{lab}} = \frac{1}{32(2\pi)^5 m_d\, p}\frac{k_{\alpha\mathrm{lab}}^2}{\omega_{\alpha\mathrm{lab}}}\int\frac{\mathrm{d}^3k_1}{\omega_1}\frac{\mathrm{d}^3k_2}{\omega_2}|\mathcal{M}|^2\,\delta^4(p_1+p_2-k_1-k_2-k_\alpha). \quad (3.2)$$

The remaining integrand in eq. (3.2) is relativistically invariant and the resultant integral is most easily evaluated in the $\pi\pi$ rest frame, where the pions

go back to back. Denoting with an asterisk quantities evaluated in this frame, a straightforward calculation gives

$$\mathcal{I} = \int \frac{\mathrm{d}^3k_1^*}{\omega_1^*}\frac{\mathrm{d}^3k_2^*}{\omega_2^*}|\mathcal{M}^*|^2\,\delta^3(\mathbf{k}_1^*+\mathbf{k}_2^*)\,\delta(M_X-\omega_1^*-\omega_2^*) = \frac{k^*}{M_X}\int d\Omega^*|\mathcal{M}^*|^2. \quad (3.3)$$

The missing mass M_X in the $dd \to \alpha X$ reaction is, in our model, the effective mass of the pion-pion system $m_{\pi\pi}$. In terms of this and $\mathbf{k}^* = \frac{1}{2}(\mathbf{k}_1^* - \mathbf{k}_2^*)$, the differential cross section is

$$\left(\frac{\mathrm{d}^2\sigma}{\mathrm{d}\Omega_\alpha \mathrm{d}k_\alpha}\right)_{\mathrm{lab}} = \frac{1}{32(2\pi)^5}\,\frac{k_{\alpha\mathrm{lab}}^2 k^*}{m_d M_X p\,\omega_{\alpha\mathrm{lab}}}\int \mathrm{d}\Omega^*\,\frac{1}{9}\sum_{\mathrm{spin,pol.}}|\mathcal{M}^*|^2, \quad (3.4)$$

where the averaging over the initial spins and summing over the final is now included.

The description has so far concentrated on $\pi^+\pi^-$ production. Simple isospin arguments suggest that $\pi^0\pi^0$ production should be exactly half that of the charged pion but the narrowness of the ABC peak and the significant pion mass differences make it necessary to evaluate the kinematics separately in the two cases.

3.1.1 Transformation to the $\pi\pi$ rest frame

In order to implement the phase space considerations of the previous section, the matrix element has to be expressed in the $\pi\pi$ rest frame so that a Lorentz transformation is needed between the CM and $\pi\pi$ systems. Since in general the α-particle emerges at an arbitrary angle θ_{CM} with respect to the beam direction, this involves a rotation. The righthanded CM coordinate system is oriented with its z-axis in the beam direction ($\hat{\mathbf{p}}$), the x-axis in the plane spanned by $\hat{\mathbf{p}}$ and the α-particle momentum ($\mathbf{k}_\alpha$), and the y-axis parallel to $\hat{\mathbf{p}} \times \hat{\mathbf{k}}_\alpha$. A new coordinate system is introduced, by rotating about the y-axis, such that the new z-axis coincides with the α-particle direction. A Lorentz boost is then applied in the α-particle direction so that, in the new system, the pions emerge back to back. Explicitly this gives

$$\begin{aligned}
\frac{1}{2}(\omega_1 - \omega_2) &= -\frac{k_\alpha k_{z'}^*}{m_{\pi\pi}} && (3.5)\\
\frac{1}{2}(k_1^x - k_2^x) &= k_{x'}^*\cos\theta_{\mathrm{CM}} + \gamma_\pi k_{z'}^*\sin\theta_{\mathrm{CM}} && (3.6)\\
\frac{1}{2}(k_1^y - k_2^y) &= k_{y'}^* && (3.7)\\
\frac{1}{2}(k_1^z - k_2^z) &= -k_{x'}^*\sin\theta_{\mathrm{CM}} + \gamma_\pi k_{z'}^*\cos\theta_{\mathrm{CM}}, && (3.8)
\end{aligned}$$

where xyz refer to the CM, and $x'y'z'$ to the $\pi\pi$ systems and $\gamma_\pi = (\omega_1+\omega_2)/m_{\pi\pi}$ is the Lorentz boost factor between the two. The transverse and longitudinal components of the pion momentum difference become

$$\tfrac{1}{2}\,|\mathbf{k}_1^b - \mathbf{k}_2^b| = \left[(k^*_{x'}\cos\theta_{\rm CM} + \gamma_\pi k^*_{z'}\sin\theta_{\rm CM})^2 + (k^*_{y'})^2\right]^{\frac{1}{2}} \quad (3.9)$$

$$\tfrac{1}{2}\,(k_1^z - k_2^z) = -k^*_{x'}\sin\theta_{\rm CM}, +\gamma_\pi k^*_{z'}\cos\theta_{\rm CM} \quad (3.10)$$

where b indicates directions perpendicular to the beam.

3.2 Vertex parametrizations

3.2.1 Split-up vertices

Since large Fermi momenta are not required in our model, we shall only retain the dominant S-state parts of the nuclear wave functions. In a non-relativistic pole model the d:pn vertices may be parametrized as:

$$M_{d_i} = \left(\frac{-1}{\sqrt{2}}\boldsymbol{\sigma}\cdot\boldsymbol{\epsilon}_i\right)(2\pi)^{3/2}\frac{\sqrt{2m_d}}{m}(\mathbf{q}_i^2 + \alpha_d^2)\varphi(\mathbf{q}_i') \quad (3.11)$$

where $\varphi(\mathbf{q})$ is the deuteron S-state wave function in momentum space, $\mathbf{q}_i' \equiv (\mathbf{q}_i^b, q_i^z/\gamma)$ the relative momentum of the nucleons, boosted in the z-direction to take the relativistic motion into account, and $\boldsymbol{\epsilon}_i$ the deuteron polarization vector. The parameter $\alpha_d = \sqrt{mB_d}$, where m is the nucleon mass and B_d the deuteron binding energy.

The dd:α vertex is parametrized in a similar manner by

$$M_\alpha = \left(\frac{-1}{\sqrt{3}}\boldsymbol{\epsilon}\cdot\boldsymbol{\epsilon}'\right)(2\pi)^{3/2}2\sqrt{2m_\alpha}(\mathbf{q}_\alpha^2 + \alpha^2)\psi^\dagger(\mathbf{q}_\alpha), \quad (3.12)$$

where $\boldsymbol{\epsilon}$ and $\boldsymbol{\epsilon}'$ are the deuteron polarization vectors, $\psi(\mathbf{q}_\alpha)$ is the α:dd S-state wave function in momentum space, $\mathbf{q}_\alpha = \mathbf{q}_1 - \mathbf{q}_2 - \frac{1}{2}(\mathbf{k}_1 - \mathbf{k}_2)$ is the relative momentum of the deuterons, and $\alpha^2 = m_d B_\alpha$, with B_α being the α-particle binding energy. Due to the large mass of the α-particle and the relatively low pion momenta, there is no need to consider a Lorentz contraction factor in this case.

3.2.2 Pion production vertices

The matrix element for the free $NN \to d\pi$ reaction is expressed in terms of the partial wave amplitudes given in the appendix;

$$M_{\pi_i} = K_i \mp \boldsymbol{\sigma}\cdot\boldsymbol{Q}_i, \quad (3.13)$$

where K_i is the sum over all initial spin-singlet amplitudes and $\boldsymbol{\sigma}\cdot\mathbf{Q}_i$ is the sum over all triplet amplitudes. Note that, since we are now using $NN \to d\pi$ rather than $\pi d \to NN$, the deuteron polarization vectors should be charge-conjugated

compared to those in the appendix. The $\mp$ signs for the triplet terms, referring to the upper and lower vertices of Fig. 1 arise from the inversion of the direction of the incident nucleon momenta in the two cases. The values of the amplitudes were calculated from the SAID database [21] using the normalization discussed in the appendix. As seen in Fig. 2, the nine amplitudes retained in the appendix reproduce the SAID predictions for the $\pi^+ d \to pp$ differential cross section to within a few percent. For comparison the cross section calculated purely with the ${}^1D_2p$ amplitude, renormalized to fill the forward cross section, is also shown. This single amplitude, which was used in our preliminary study [19], shows the manifest pion p-wave dominance which is the main origin for the ABC enhancement in our model.

In addition to considering far more input amplitudes, in the present analysis we retain also the explicit energy dependence prescribed by the database (see Sec. 4); in the earlier work we extracted the threshold k factor and then assumed a constant reduced amplitude. The energy dependence of the ${}^1D_2p$ amplitude is hence different in the two analyses.

3.3 Matrix element

The matrix element deduced from the Feynman diagram of Fig. 1 involves integration over two Fermi momenta

$$\mathcal{M} = \int \frac{\mathrm{d}^4 q_1}{(2\pi)^4} \frac{\mathrm{d}^4 q_2}{(2\pi)^4} M_{\mathrm{tot}} \,, \tag{3.14}$$

where M_{tot} is composed of the non-relativistic reduced vertex functions and the propagators stripped of their spin structure. In an order suggested by the diagram,

$$M_{\mathrm{tot}} = \sum_{\text{int. spins}} M_\alpha P_d P_{d'} \mathrm{Tr}\left(M_{d_2} P_2^c M_{\pi_1} P_4 M_{d_1} P_3^c M_{\pi_2} P_1\right), \tag{3.15}$$

where P_i are the propagators, M_x the matrix elements representing the vertices and the sum is over the spins and polarizations of the internal particles. Moreover, c denotes charge conjugation.

3.3.1 Approximation of propagators

The denominators of the nucleon propagators are factorized to make the pole structure explicit:

$$P_{1,4} = \frac{i\,2m}{(q_{20,10} + p_0 - i\epsilon)[q_{20,10} - (\alpha_d^2 + \mathbf{q}_{2,1}^2 \pm \mathbf{p}\cdot\mathbf{q}_{2,1})/p_0 + i\epsilon]} \tag{3.16}$$

$$P_{2,3}^c = \frac{-i\,2m}{(q_{20,10} - p_0 + i\epsilon)[q_{20,10} + (\alpha_d^2 + \mathbf{q}_{2,1}^2 \mp \mathbf{p}\cdot\mathbf{q}_{2,1})/p_0 - i\epsilon]}. \tag{3.17}$$

Since the Fermi momenta ($\mathbf{q}_i$) are generally quite small compared to the incident deuteron momenta, only the poles closest to the origin at $q_{10,20} = \frac{1}{p_0}(\alpha_d^2 + \mathbf{q}_{1,2}^2 \mp \mathbf{p}\cdot\mathbf{q}_{1,2})$ yield significant contributions. The integrations over q_{20} and q_{10} are then done by contour integration in the lower half plane, yielding

$$\int \frac{\mathrm{d}q_{20}\,\mathrm{d}q_{10}}{(2\pi)^2}\, P_2^c P_4 P_3^c P_1 \to \frac{-(2m)^4}{(2p_0)^2(\mathbf{q}_1^2+\alpha_d^2)(\mathbf{q}_2^2+\alpha_d^2)} \sim \frac{-m^2}{\gamma^2(\mathbf{q}_1^2+\alpha_d^2)(\mathbf{q}_2^2+\alpha_d^2)}\,, \tag{3.18}$$

where the last step assumes that $p_0 = E_d \sim 2\gamma m$.

The deuteron propagators are

$$P_{d,d'} = \frac{i}{Q_{d,d'}^2 - m_d^2 + i\epsilon}, \tag{3.19}$$

where $Q_{d,d'} = [p_0 \pm (q_{10} - q_{20}) - \omega_{1,2}, \pm(\mathbf{q}_1 - \mathbf{q}_2) - \mathbf{k}_{1,2}]$. Since $\mathbf{q}_\alpha^2 + \alpha^2 \sim -\frac{1}{2}(Q_d^2 - m_d^2 + Q_{d'}^2 - m_d^2)$, the product of the deuteron propagators and the $dd{:}\alpha$ vertex reduces to

$$M_\alpha P_d P_{d'} = \left(\frac{-1}{\sqrt{3}}\boldsymbol{\epsilon}\cdot\boldsymbol{\epsilon}'\right)(2\pi)^{\frac{3}{2}}\sqrt{2m_\alpha}\left(\frac{1}{Q_d^2 - m_d^2 + i\epsilon} + \frac{1}{Q_{d'}^2 - m_d^2 + i\epsilon}\right)\psi_\alpha^\dagger\,. \tag{3.20}$$

The denominators in this expression can be expanded as

$$\begin{aligned} Q_{d,d'}^2 - m_d^2 &= [E_d - \omega_{1,2} \pm (q_{10} - q_{20})]^2 - \left[\pm(\mathbf{q}_1 - \mathbf{q}_2) - \mathbf{k}_{1,2} - m_d^2\right]^2 \\ &\sim \mp 2m_d\left[\mathbf{v}_d\cdot(\mathbf{q}_1 + \mathbf{q}_2) + \frac{1}{2}(\omega_1 - \omega_2)\right]. \end{aligned} \tag{3.21}$$

In the last step, the relation

$$q_{10} - q_{20} = -\frac{1}{p_0}[\mathbf{p}\cdot(\mathbf{q}_1 + \mathbf{q}_2) - \mathbf{q}_1^2 + \mathbf{q}_2^2] \sim -\mathbf{v}_d\cdot(\mathbf{q}_1 + \mathbf{q}_2) \tag{3.22}$$

has been used, while quadratic terms were neglected. Using these linearized forms, the principal value terms cancel in the sum of propagators in eq. (3.20) to leave only a δ-function term;

$$M_\alpha P_d P_{d'} = \left(\frac{-1}{\sqrt{3}}\boldsymbol{\epsilon}\cdot\boldsymbol{\epsilon}'\right)(2\pi)^{\frac{3}{2}}\sqrt{2m_\alpha}\psi_\alpha^\dagger\frac{-i\pi}{m_d v_d}\delta\left(q_1^z + q_2^z + \frac{\omega_1 - \omega_2}{2v_d}\right)\,. \tag{3.23}$$

Assuming that Fermi momentum effects may be neglected in the spin couplings, which is a good approximation in the ABC peak regions, the matrix element is written as the product

$$\mathcal{M} \equiv -i\frac{m_\alpha}{v_d}\mathcal{W}\,\mathcal{K}, \tag{3.24}$$

where the spin kernel $\mathcal{K}$ and dimensionless scalar form factor $\mathcal{W}$ are given, respectively, by

$$\mathcal{K} \equiv \sum_{\text{int. spins}} \frac{-1}{\sqrt{3}} \boldsymbol{\epsilon} \cdot \boldsymbol{\epsilon}' \text{Tr} \left[\left(\frac{-\boldsymbol{\sigma} \cdot \boldsymbol{\epsilon}_2}{\sqrt{2}} \right) (K_1 - \boldsymbol{\sigma} \cdot \mathbf{Q}_1) \left(\frac{-\boldsymbol{\sigma} \cdot \boldsymbol{\epsilon}_1}{\sqrt{2}} \right) (K_2 + \boldsymbol{\sigma} \cdot \mathbf{Q}_2) \right] , \tag{3.25}$$

and

$$\mathcal{W} \equiv \frac{1}{\sqrt{\pi m_\alpha}} \int \frac{\mathrm{d}^3 q_1 \mathrm{d}^3 q_2}{\gamma^2} \varphi_d(\mathbf{q}_1') \varphi_d(\mathbf{q}_2') \psi_\alpha^\dagger(\mathbf{q}_\alpha) \, \delta\Big(q_1^z + q_2^z + \frac{\omega_1 - \omega_2}{2 v_d} \Big) \cdot \tag{3.26}$$

3.4 Summing over spins and polarizations

The spin kernel of eq. (3.25) can be simplified somewhat by expanding the product and taking the trace. This results in the spin-decoupled form

$$\mathcal{K} = \frac{-1}{\sqrt{3}} \left[\mathcal{A} (\boldsymbol{\epsilon}_1 \cdot \boldsymbol{\epsilon}_2) - i \overline{\mathcal{B}} \cdot (\boldsymbol{\epsilon}_1 \times \boldsymbol{\epsilon}_2) - \boldsymbol{\epsilon}_1 \cdot \overline{\overline{\mathcal{C}}} \cdot \boldsymbol{\epsilon}_2 \right] , \tag{3.27}$$

where the spin-0, -1, and -2 amplitudes are

$$\mathcal{A} \equiv \sum_{\text{pol.}} (\boldsymbol{\epsilon} \cdot \boldsymbol{\epsilon}') \left(K_1 K_2 + \tfrac{1}{3} \mathbf{Q}_1 \cdot \mathbf{Q}_2 \right) \tag{3.28}$$

$$\overline{\mathcal{B}} \equiv \sum_{\text{pol.}} (\boldsymbol{\epsilon} \cdot \boldsymbol{\epsilon}') \left(K_1 \mathbf{Q}_2 + K_2 \mathbf{Q}_1 \right) \tag{3.29}$$

$$\overline{\overline{\mathcal{C}}} \equiv \sum_{\text{pol.}} (\boldsymbol{\epsilon} \cdot \boldsymbol{\epsilon}') \left(\mathbf{Q}_1 \mathbf{Q}_2 + \mathbf{Q}_2 \mathbf{Q}_1 - \tfrac{2}{3} \mathbf{Q}_1 \cdot \mathbf{Q}_2 \right) \tag{3.30}$$

and the sums are over the polarizations of the internal deuterons.

The unpolarized matrix element squared is then

$$\sum_{\text{ext. pol.}} |\mathcal{K}|^2 = \tfrac{1}{3} \left(3 |\mathcal{A}|^2 + 2 |\overline{\mathcal{B}}|^2 + |\overline{\overline{\mathcal{C}}}|^2 \right) , \tag{3.31}$$

where $|\overline{\overline{\mathcal{C}}}|^2 \equiv \sum_{i,j} \mathcal{C}_{ij} \mathcal{C}_{ij}^\dagger$ and the sum is over the polarizations of the external deuterons. The deuteron vector and tensor analyzing powers A_y and A_{yy} are obtained from the sums

$$\sum_{i,j,k} \mathcal{K}_{ij} P_{jk} \mathcal{K}_{ik}^\dagger , \tag{3.32}$$

where the P_{ij} are the spin projection operators in a Cartesian basis [22]. Since the dominant ${}^1D_2 p$ amplitude by itself gives only a contribution to the $\mathcal{A}$ amplitude, this would lead to $A_y = A_{yy} = 0$. The analyzing powers are therefore very sensitive probes of the importance of non-dominant $NN \to d\pi$ input amplitudes.

To avoid the tedious algebra associated with nine partial wave amplitudes occurring bilinearly in each *amplitude*, the above sums and contractions were in practice carried out numerically.

3.5 Form factor in configuration space

The form factor of eq. (3.26) is most easily evaluated by transforming to configuration space;

$$\begin{aligned}\mathcal{W} &= \frac{1}{\sqrt{2m_\alpha}}\int \mathrm{d}^2b\,\mathrm{d}z_1\mathrm{d}z_2\,\Phi_d(\mathbf{b},\gamma z_1)\Phi_d(-\mathbf{b},\gamma z_2)\Psi^\dagger_\alpha(\mathbf{x}_\alpha) \\ &\times \exp\Big[-\frac{i}{2}(\mathbf{k}_1-\mathbf{k}_2)\cdot\mathbf{x}_\alpha\Big]\,\exp\Big[-\frac{i}{4v_d}(\omega_1-\omega_2)(z_1+z_2)\Big]\,, \qquad (3.33)\end{aligned}$$

where $\mathbf{x}_\alpha = (\mathbf{b},(z_1-z_2)/2)$.

Since the wave functions have been taken to be spherically symmetric, the angular integration over the b variable can be performed explicitly. Furthermore, only the even parts of the exponentials will contribute, so that

$$\begin{aligned}\mathcal{W} = \frac{2\pi}{\sqrt{2m_\alpha}}\int b\,\mathrm{d}b\,\mathrm{d}z_1\mathrm{d}z_2\,\Phi_d(\mathbf{b},\gamma z_1)\,\Phi_d(-\mathbf{b},\gamma z_2)\,\Psi^\dagger_\alpha\Big(\mathbf{b},\frac{z_1-z_2}{2}\Big) \\ \times\; J_0\Big(\tfrac{1}{2}|\mathbf{k}_1^b-\mathbf{k}_2^b|b\Big)\cos\Big[\tfrac{1}{4}(k_1^z-k_2^z)(z_1-z_2)\Big]\cos\Big[\tfrac{1}{4v_d}(\omega_1-\omega_2)(z_1+z_2)\Big] \qquad (3.34)\end{aligned}$$

3.6 Reduction of cross sections due to flux damping

The fluxes of initial and final particles are reduced because of multiple scattering. Any detailed microscopic estimate of such effects would rest upon assumptions that are difficult to justify quantitatively. For example, in any Glauber-like approximation, correlation effects would be very large for the light nuclei that we are considering. We therefore limit our ambition, attempting a crude estimate through an overall scale factor. This should at least give a hint of the magnitude and direction of the damping. Since our model is based upon two $NN \to d\pi$ reactions, it is natural to estimate the reduction in flux through the factor

$$\mathcal{D} = \frac{\sigma_{\rm tot}(dd)}{2[\sigma_{\rm tot}(pn)+\sigma_{\rm tot}(pp)]}\times\left(\frac{\sigma_{\rm tot}(\pi\alpha)}{2\sigma_{\rm tot}(\pi d)}\right)^2, \qquad (3.35)$$

where the last factor is squared since there are two emerging pions.

The assumption behind this formula is that in the initial state the flux reduction due to multiple scattering is the same in all dd reaction. A similar argument is valid in the final state, assuming the α-particle to be a dd aggregate. The values of total cross sections needed were taken from [23] (NN), [24] (dd), [25] (πd), and [26] ($\pi\alpha$). Interpolation between different data sets was often needed and the values used are collected in Table 1, together with the calculated reduction $\mathcal{D}$. The latter is compared to the factor needed to scale our model calculations to fit the data, as shown in the figures. While our simplistic estimate goes in the right direction, it does not account for all the deviations from the data. There is however considerable uncertainty in the pion distortion at the lower energies.

4 Numerical calculation

The evaluation of cross sections and polarization observables was done in two steps. The form factor of eq. (3.34) was firstly obtained using standard Gauss-Legendre routines with 50 points in each of the three dimensions and tabulated in steps of the parameters $k_{\alpha\mathrm{lab}}$, φ^*, and $\cos\theta^*$. In the second step the spin sums and contractions were done at each of these points, followed by the integration over phase space, including the tabulated form factor.

4.1 Wave functions

The S-state Paris [27] wave function is used to describe the deuterons, whereas the α-particle is represented by the dd:α cluster function of Forest et al. [28]. It is shown in the latter work that the nucleon-nucleon distributions in the α-particle and the deuteron are very similar for short distances ($r < 2$ fm), with a constant scale factor of 4.7 between them. Since pion absorption on deuterons occurs mainly when the nucleons are close together, we need the number N_α of pairs of such "small" deuterons in the α-particle. Assuming the neutron-proton distribution inside the two deuterons of the α-particle to be independent of each other, we therefore normalize the wave function to $N_\alpha = 2.3$.

Since the shape of the α:dd function is similar to a Gaussian, $\exp(-\beta^2 r^2)$, it is easy to test our dependence on it by varying the parameter β. The result of this test (using the constant amplitudes of next section) at $T_d = 1250$ MeV and $\theta_\alpha = 0.3^\circ$ is shown in Fig. 3. While the ABC peaks remain largely unaffected, there is large sensitivity in the central region. Calculations at 11.0° and also at 787 MeV show less variation. Hence this uncertainty is associated with high missing masses.

4.2 Partial wave amplitudes

The values of the partial wave amplitudes can be extracted from the SAID database [21] in several ways. The first and simplest is to use constant amplitudes evaluated at the kinematics corresponding to the edges of the spectra, i.e. close to the ABC peaks, where the two pions have identical momenta. The single amplitude used in our previous work was extracted in this way [19].

Energy dependent input — where the amplitudes are calculated separately for each point of integration — is an attempt to take the Fermi motion in the α-particle into account. There is no unambiguous way to do this and so we have adopted two slightly different methods. One based on the previous technique, but calculated at each point separately, will be called the E1 prescription. The second approach (E2) uses the same pion momenta but now assumes the deuterons to have half the α-particle momentum. The two clearly coincide at the edges of

the missing mass spectra, but have different characteristics in the central region. Their relative merits will be discussed in the next section.

5 Results

The predictions of our model are compared with the Saclay unpolarized cross section data of Ref. [6] in Figs 4 and 5. Shown are the raw results from the E2 prescription and also those obtained by smearing E1 and E2 over a Gaussian experimental resolution in the α-particle momentum with a relative standard deviation $\sigma(k_\alpha)/k_\alpha = 0.5\%$ [6]. The calculations are scaled to fit the data with factors listed in Table 1. This scaling is independent of the choice of amplitudes. The agreement with data is remarkably good, both in angular distribution and energy dependence. The differences found between the scale factors and the flux damping estimates could be attributed mainly to the crudeness of the estimate and the uncertainties in its input data.

The slight discrepancy at the central bump for small angles could be due to the production of three pions or to our simplified treatment of the Fermi momenta. A broad σ-meson [23] would also enhance the cross section here. An estimate of the possible contribution from production of η-mesons could be obtained from a measurement at 1.95 GeV [29]. The cross section is however so low ($\sim$ 1 μb/(srGeV/c)) that it should be invisible in all the plots, except possibly for 1.94 GeV where one might see a hint of a peak. As illustrated in Fig. 3, the central region is also sensitive to the precise form assumed for the α-particle wave function. Inclusion of D-states in the wave functions would give effects for large missing mass as well since it corresponds to large Fermi momenta.

Apart from a small change in the ABC peaks, the main difference between E1 and E2 is found in the central region. The reason for this is the different kinematics used in the two cases — E1 tends to overstate the πd energy in the central bump and thus attains the maximal $NN \to d\pi$ cross section already at 940 MeV, while E2 has its maximum at 1250 MeV. This accounts for the E1 overestimating (compared to E2) at low missing masses and underestimating at high maximal missing mass. At 1250 MeV and 11.0° the missing mass is not high enough to be sensitive to the difference between the two assumptions. Unfortunately the range of data in the SAID database [21] does not extend to the energies needed for E1 at 1412 MeV and for E2 at 1938 MeV. The close agreement between E2 and the calculation with constant amplitudes at 1412 MeV justifies the use of constant amplitudes at the higher energies in Fig. 5.

The underestimate at 787 MeV is probably an indication of a more severe problem within our double-Δ model. There are two measurements at even lower energies, one close to threshold at $T_d = 570$ MeV [13] and another at 650 MeV [12]. In both cases the data are structureless, and consistent with pure phase space, with total cross sections of $\sigma(570) \sim 43$ nb and $\sigma(650) \sim 600$ nb, respectively.

In our model a pronounced ABC-like structure should be clearly visible at both energies. However, our predicted total cross sections are a factor of about 20 too low and it therefore seems that there is some other mechanism which is mainly responsible for the smooth behavior near threshold. This extra contribution might account already for our underestimate at 787 MeV.

The deuteron analyzing powers measured by the SPESIII spectrometer at Saturne [7] are seen in Fig. 6 together with our model predictions integrated over the spectrometer acceptance. The slope of vector analyzing power A'_y in the forward direction is calculated according to the experimental average procedure described in Ref. [7]. The differences between the E1 and E2 calculations are clearly seen for A'_y, while they are rather marginal for A_{yy}. This greater sensitivity of A'_y could be due to its dependence upon the relative phase between singlet and triplet amplitudes and also the importance of the strongly energy-dependent and dominant ${}^1D_2p$ amplitude. The E1 predictions are shifted by an arbitrary -2 rad^{-1} in the figure to show the close resemblance to the data structures. Any small extra terms in the amplitude could cause such a shift. For both analyzing powers, there are again discrepancies in the central region, presumably for the same reasons as for the unpolarized cross sections.

All calculations were done using the C500 solution of [21] but, in order to check the stability of the result, they were repeated for the SP96 solution as well. The two sets of results are very close and the small differences found are completely overshadowed by the larger uncertainties inherent in the procedures for extracting amplitudes.

6 Conclusions

For the first time a quantitative model has been proposed for the ABC effect in the $dd \to \alpha X$ reaction. Despite its simplicity, and without benefitting from any free parameters, it is able to reproduce all the main features of the α-particle momentum spectrum observed throughout the double-Δ region. It is hence clear that, at least for this reaction, the ABC effect is indeed a kinematical enhancement in the independent production of two p-wave pions when these emerge with parallel momenta.

The analyzing power predictions are equally impressive and reproduce quite nicely the frequency and strength of the oscillations for both A_{yy} and A'_y. Since these quantities are sensitive to the non-dominant input amplitudes, and in particular their relative phases, this more thorough examination of the details of our model adds further strength to the conclusion that it supplies the correct dynamics in the double-Δ region.

The low energy data present, however, a more delicate situation to interpret. We do not think that it is possible to force the present model to reproduce pure phase space at low energies. Since the p-wave dominance of $NN \to d\pi$ extends

almost down to threshold, the s-wave pions needed to furnish isotropy could not be produced via that subprocess. The analogous contribution of isovector nucleon-nucleon pairs, in for example $pp \to pp\pi^0$, is known to be much smaller than isoscalar pairs both near threshold and throughout the Δ-peak [30]. There must therefore be another production mechanism present, which is dominant at low energies but which assumes lesser importance at higher energies where the ABC is seen clearly. In order to improve our understanding of the dynamics in this kinematical region, we suggest that further experiments should be done at deuteron beam energies $T_d < 0.8$ GeV. In addition to inclusive polarized and unpolarized cross sections, exclusive reactions are also needed so that angular distributions of pairs of the final particles can be constructed. Such data already exist for $pd \to {}^3\mathrm{He}\,\pi^+\pi^-$ [11]. Since all such quantities can be calculated within our model they provide extra confirmations and tests of it.

Given its quantitative success it is natural to ask if our model could be extended to include other reactions as well. A simple extension would be to calculate the double photon production $dd \to \alpha\gamma\gamma$ via two $np \to d\gamma$ reactions. This could be an important background in the measurement of the charge-symmetry-breaking $dd \to \alpha\pi^0$ reaction, observed at Saturne in the double-Δ region [31]. We are currently investigating this possibility.

Acknowledgement

We would like to thank Pia Thörngren Engblom of the Stockholm Nuclear Physics Group whose experiment at the Celsius ring [13] was the starting point for this study. This work has been made possible by the continued financial support of the Swedish Royal Academy and the Swedish Research Council, and one of the authors (CW) would like to thank them and The Svedberg Laboratory for their generous hospitality.

A Partial wave amplitudes and Clebsch-Gordan coefficients expressed by spin amplitudes

We find it simpler to estimate the double-Δ contribution to the two-pion production using a spin-amplitude description of the $\pi^+ d \to pp$ reaction rather than employing partial waves. We therefore give here expressions for the lower partial waves in terms of the Pauli spin matrices ($\boldsymbol{\sigma}$), the deuteron polarization vectors ($\boldsymbol{\epsilon}$), and the proton and pion momenta ($\mathbf{p}$ and $\mathbf{k}$). The partial waves are denoted by $^{2S_{pp}+1}(L_{pp})_J l_\pi$, where S_{pp} and L_{pp} are the spin and orbital angular momentum of the proton-proton system in the initial state, J is the total angular momentum, and l_π is the pion angular momentum in the final state. The operators $\mathcal{O}_i$ corresponding to particular partial wave transitions are given below in the normalization $\int \mathrm{d}\Omega \sum_{\boldsymbol{\epsilon}} \mathrm{Tr}|\mathcal{O}_i|^2 = 2 \cdot 4\pi(2J_i+1)$.

A.1 Singlet amplitudes

$$\mathcal{O}\left({}^1S_0 p\right) = -\hat{\mathbf{k}} \cdot \boldsymbol{\epsilon} \tag{A.1}$$

$$\mathcal{O}\left({}^1D_2 p\right) = \sqrt{\frac{5}{2}} \left\{ 3(\hat{\mathbf{p}} \cdot \hat{\mathbf{k}})(\hat{\mathbf{p}} \cdot \boldsymbol{\epsilon}) - \hat{\mathbf{k}} \cdot \boldsymbol{\epsilon} \right\} \tag{A.2}$$

$$\mathcal{O}\left({}^1D_2 f\right) = \frac{\sqrt{15}}{2} \left\{ 2(\hat{\mathbf{p}} \cdot \hat{\mathbf{k}})(\hat{\mathbf{p}} \cdot \boldsymbol{\epsilon}) - \left[5(\hat{\mathbf{p}} \cdot \hat{\mathbf{k}})^2 - 1 \right] \hat{\mathbf{k}} \cdot \boldsymbol{\epsilon} \right\} \tag{A.3}$$

$$\begin{aligned} \mathcal{O}\left({}^1G_4 f\right) &= \frac{3}{4} \Big\{ 35(\hat{\mathbf{p}} \cdot \hat{\mathbf{k}})^3 (\hat{\mathbf{p}} \cdot \boldsymbol{\epsilon}) + 3(\hat{\mathbf{k}} \cdot \boldsymbol{\epsilon}) \\ &- 15 \left[(\hat{\mathbf{p}} \cdot \hat{\mathbf{k}})^2 (\hat{\mathbf{k}} \cdot \boldsymbol{\epsilon}) + (\hat{\mathbf{p}} \cdot \hat{\mathbf{k}})(\hat{\mathbf{p}} \cdot \boldsymbol{\epsilon}) \right] \Big\} \end{aligned} \tag{A.4}$$

A.2 Triplet amplitudes

$$\mathcal{O}\left({}^3P_1 s\right) = \sqrt{\frac{3}{2}} i \boldsymbol{\epsilon} \cdot (\hat{\mathbf{p}} \times \boldsymbol{\sigma}) \tag{A.5}$$

$$\mathcal{O}\left({}^3P_1 d\right) = -\frac{\sqrt{3}}{2} i \left\{ 3(\hat{\mathbf{k}} \cdot \boldsymbol{\epsilon}) \hat{\mathbf{k}} \cdot (\hat{\mathbf{p}} \times \boldsymbol{\sigma}) - \boldsymbol{\epsilon} \cdot (\hat{\mathbf{p}} \times \boldsymbol{\sigma}) \right\} \tag{A.6}$$

$$\mathcal{O}\left({}^3P_2 d\right) = -\frac{\sqrt{15}}{2} i \left\{ (\hat{\mathbf{p}} \cdot \hat{\mathbf{k}}) \boldsymbol{\sigma} \cdot (\hat{\mathbf{k}} \times \boldsymbol{\epsilon}) - (\boldsymbol{\sigma} \cdot \hat{\mathbf{k}}) \hat{\mathbf{k}} \cdot (\hat{\mathbf{p}} \times \boldsymbol{\epsilon}) \right\} \tag{A.7}$$

$$\begin{aligned} \mathcal{O}\left({}^3F_2 d\right) &= \sqrt{\frac{5}{2}} i \Big\{ 5(\hat{\mathbf{p}} \cdot \hat{\mathbf{k}})(\hat{\mathbf{p}} \cdot \boldsymbol{\sigma}) \hat{\mathbf{p}} \cdot (\hat{\mathbf{k}} \times \boldsymbol{\epsilon}) \\ &- \left[(\hat{\mathbf{p}} \cdot \hat{\mathbf{k}}) \boldsymbol{\sigma} \cdot (\hat{\mathbf{k}} \times \boldsymbol{\epsilon}) + (\boldsymbol{\sigma} \cdot \hat{\mathbf{k}}) \hat{\mathbf{p}} \cdot (\hat{\mathbf{k}} \times \boldsymbol{\epsilon}) \right] \Big\} \end{aligned} \tag{A.8}$$

$$\begin{aligned} \mathcal{O}\left({}^3F_3 d\right) &= \frac{\sqrt{7}}{4} i \Big\{ \left[5(\hat{\mathbf{p}} \cdot \hat{\mathbf{k}})^2 - 1 \right] \boldsymbol{\epsilon} \cdot (\hat{\mathbf{p}} \times \boldsymbol{\sigma}) \\ &+ 10(\hat{\mathbf{p}} \cdot \hat{\mathbf{k}})(\hat{\mathbf{p}} \cdot \boldsymbol{\epsilon}) \hat{\mathbf{k}} \cdot (\hat{\mathbf{p}} \times \boldsymbol{\sigma}) - 2(\hat{\mathbf{k}} \cdot \boldsymbol{\epsilon}) \hat{\mathbf{k}} \cdot (\hat{\mathbf{p}} \times \boldsymbol{\sigma}) \Big\} \end{aligned} \tag{A.9}$$

A.3 Clebsch-Gordan coefficients

In the $\boldsymbol{\sigma}$-$\boldsymbol{\epsilon}$ expressions for Clebsch-Gordan coefficients, the non-relativistic two-component spinor η and its charge conjugate $\eta_c \equiv -i\sigma^2\eta^*$ are introduced.

$$\left\langle 1\lambda \left| \frac{1}{2}m_1 \, \frac{1}{2}m_2 \right\rangle \right. \;\leftrightarrow\; \eta_{c1}^\dagger \left(\frac{-1}{\sqrt{2}} \boldsymbol{\sigma}\cdot\boldsymbol{\epsilon}^{(\lambda)\dagger} \right) \eta_2 \tag{A.10}$$

$$\left\langle \frac{1}{2}m_1 \, \frac{1}{2}m_2 \right| 1\lambda \left. \right\rangle \;\leftrightarrow\; \eta_2^\dagger \left(\frac{-1}{\sqrt{2}} \boldsymbol{\sigma}\cdot\boldsymbol{\epsilon}^{(\lambda)} \right) \eta_{1c} \tag{A.11}$$

$$\left\langle \frac{1}{2}m_2 \,|\, 1\lambda \, \frac{1}{2}m_1 \right\rangle \;\leftrightarrow\; \eta_2^\dagger \left(\frac{1}{\sqrt{3}} \boldsymbol{\sigma}\cdot\boldsymbol{\epsilon}^{(\lambda)} \right) \eta_1 \tag{A.12}$$

$$\langle 00|\, 1\mu_1 1\mu_2\rangle \;\leftrightarrow\; \frac{-1}{\sqrt{3}} \boldsymbol{\epsilon}^{(\mu_1)}\cdot\boldsymbol{\epsilon}^{(\mu_2)} \tag{A.13}$$

$$\langle 1\lambda|\, 1\mu_1 1\mu_2\rangle \;\leftrightarrow\; \boldsymbol{\epsilon}^{(\lambda)\dagger}\cdot\left(\frac{-i}{\sqrt{2}} \boldsymbol{\epsilon}^{(\mu_1)}\times\boldsymbol{\epsilon}^{(\mu_2)} \right) \tag{A.14}$$

A.4 Relation to the SAID formalism

The $\boldsymbol{\sigma}$-$\boldsymbol{\epsilon}$ formalism uses the normalization

$$\frac{\mathrm{d}\bar{\sigma}}{\mathrm{d}\Omega}(\pi^+ d \to pp) = \frac{m^2}{4(2\pi)^2 s_{\pi d}} \frac{p}{k} \frac{1}{3} \sum_{\text{spins}} |\mathcal{M}|^2, \tag{A.15}$$

where $\sqrt{s_{\pi d}}$ is the cm energy. The matrix element is then of the form

$$\mathcal{M} = \left\langle pp \left| \sum_i \mathcal{A}_i \mathcal{O}_i \right| \pi^+ d \right\rangle \,, \tag{A.16}$$

where $\mathcal{A}_i$ is the complex amplitude for a particular partial wave.

In the formalism of the SAID database [21]

$$\frac{\mathrm{d}\bar{\sigma}}{\mathrm{d}\Omega}(\pi^+ d \to pp) = \frac{1}{6k^2} \sum_{i=1}^{6} |H_i|^2, \tag{A.17}$$

where the helicity amplitudes, H_i, are linear combinations of partial wave amplitudes T. The relation between the $\boldsymbol{\sigma}$-$\boldsymbol{\epsilon}$ and SAID partial wave amplitudes is then

$$\mathcal{A} = \frac{2\pi}{m} \sqrt{\frac{2s_{\pi d}}{pk}} T, \tag{A.18}$$

since all the spin-momenta structures and relative phases are incorporated in the $\boldsymbol{\sigma}$-$\boldsymbol{\epsilon}$ formulae.

References

[1] R.J. Homer, Q.H. Khan, W.K. McFarlane, J.S.C. McKee, A.W. O'Dell, L. Riddiford, P.G. Williams, and D. Griffiths, Phys. Lett. **9**, 72 (1964); J.H. Hall, T.A. Murray, and L. Riddiford, Nucl. Phys. **B12**, 573 (1969).

[2] J. Banaigs, J. Berger, J. Duflo, L. Goldzahl, M. Cottereau, and F. Lefebvres, Nucl. Phys. **B28**, 509 (1971).

[3] F. Plouin *et al.*, Nucl. Phys. **A302**, 413 (1978).

[4] A. Abashian, N.E. Booth, and K.M. Crowe, Phys. Rev. Lett. **5**, 258 (1960); N.E. Booth, and A. Abashian, Phys. Rev. **132**, 2314 (1963).

[5] J. Banaigs, J. Berger, L. Goldzahl, T. Risser, L. Vu-Hai, M. Cottereau, and C. Le Brun, Nucl. Phys. **B67**, 1 (1973).

[6] J. Banaigs, J. Berger, L. Goldzahl, L. Vu-Hai, M. Cottereau, C. Le Brun, F.L. Fabbri, and P. Picozza, Nucl. Phys. **B105**, 52 (1976).

[7] N. Willis *et al.*, Phys. Lett. **406B**, 14 (1997); R. Wurzinger *et al.*, Phys. Lett. (in press).

[8] T. Maung, G.E. Masek, E. Miller, H. Ruderman, W. Vernon, K.M. Crowe, and N.T. Dairiki, Phys. Lett. **33B**, 521 (1970).

[9] S. Weinberg, Phys. Rev. Lett. **17**, 616 (1966).

[10] C.L. Hollas, C.R. Newsom, P.J. Riley, B.E. Bonner, and G. Glass, Phys. Rev. C **25**, 2614 (1982).

[11] F. Belleman *et al.*, University of Bonn preprint (1998).

[12] K.R. Chapman *et al.*, Phys. Lett. **21**, 465 (1966).

[13] C. Bargholtz *et al.*, Phys. Lett. **398B**, 264 (1997); P. Thörngren Engblom, Ph.D. thesis, University of Stockholm, 1997.

[14] T. Risser and M.D. Shuster, Phys. Lett. **43B**, 68 (1973); I. Bar-Nir, T. Risser, and M.D. Shuster, Nucl. Phys. **B87**, 109 (1975); C.A. Mosbacher and F. Osterfeld, *Proceedings of the Baryon98 Conference*, (World Scientific, Singapore), (in press).

[15] J.C. Anjos, D. Levy, and A. Santoro, Nuovo Cimento **33**A, 23 (1976).

[16] G.W. Barry, Nucl. Phys. **B85**, 239 (1975).

[17] G. Kälbermann and J.M. Eisenberg, Nucl. Phys. **A426**, 599 (1984).

[18] L. Alvarez-Ruso, http://xxx.lanl.gov/abs/nucl-th/9811058

[19] A. Gårdestig, G. Fäldt, and C. Wilkin, Phys. Lett. **421B**, 41 (1998).

[20] J.D. Bjorken and S.D. Drell, *Relativistic Quantum Mechanics*, (McGraw-Hill, New York, 1964).

[21] R.A. Arndt, I.I. Strakovsky, R.L. Workman, and D.V. Bugg, Phys. Rev. C **48**, 1926 (1993); http://said.phys.vt.edu/said_branch.html/

[22] The Madison Convention, in *Proceedings of the 3rd International Symposium on Polarization Phenomena in Nuclear Reactions, 1970,* edited by H.H. Barschall and W. Haeberli, (University of Wisconsin, Madison, 1970) p. *xxv.*

[23] C. Caso *et al.*, Eur. Phys. J. **C3**, 1 (1998).

[24] T. Kishida *et al.*, Phys. Rev. C **41**, 180 (1990).

[25] E. Pedroni *et al.*, Nucl. Phys. **A300**, 321 (1978).

[26] E.C. Fowler, W.B. Fowler, R.P. Shutt, A.M. Thorndike, and W.L. Whittemore, Phys. Rev. **91**, 135 (1953); Y.A. Budagov, P.F. Ermolov, E.A. Kushnirenko, and V.I. Moskalev, Zh. Eksp. Teor. Fiz. **42**, 1191 (1961) [Sov. Phys. JETP, **15**, 824 (1962)]; M.S. Kozodaev, M.M. Kulyukin, R.M. Sulyaev, A.I. Filippov, and Y.A. Schcherbakov, Zh. Eksp. Teor. Fiz. **38**, 409 (1960) [Sov. Phys. JETP **11**, 300 (1960)]; C. Wilkin, C.R. Cox, J.J. Domingo, K. Gabathuler, E. Pedroni, J. Rohlin, P. Schwaller, and N.W. Tanner, Nucl. Phys. **B62**, 61 (1973); P. Chavanon, M. Crozon, T. Leray, J.L. Narjoux, and Z. Marie, Nuovo Cimento **40A**, 935 (1965).

[27] M. Lacombe, B. Loiseau, R. Vinh Mau, J. Côté, P. Pirés, and R. de Tourreil, Phys. Lett. **101B**, 139 (1981).

[28] J.L. Forest, V.R. Pandharipande, S.C. Pieper, R.B. Wiringa, R. Schiavilla, and A. Arriaga, Phys. Rev. C **54**, 646 (1996); http://www.phy.anl.gov/theory/research/overlap/

[29] J. Banaigs *et al.*, Phys. Rev. C **32**, R1448 (1985).

[30] see for example: H. Hahn, A. Altman, D. Ashery, G. Gefen, D.R. Gill, R.R. Johnson, R. Levy-Nathansohn, M.A. Moinester, M. Sevior, and R.P. Trelle, Phys. Rev. C **53**, 1074 (1996).

[31] L. Goldzahl, J. Banaigs, J. Berger, F.L. Fabbri, J. Hüfner, and L. Satta, Nucl. Phys. **A533**, 675 (1991).

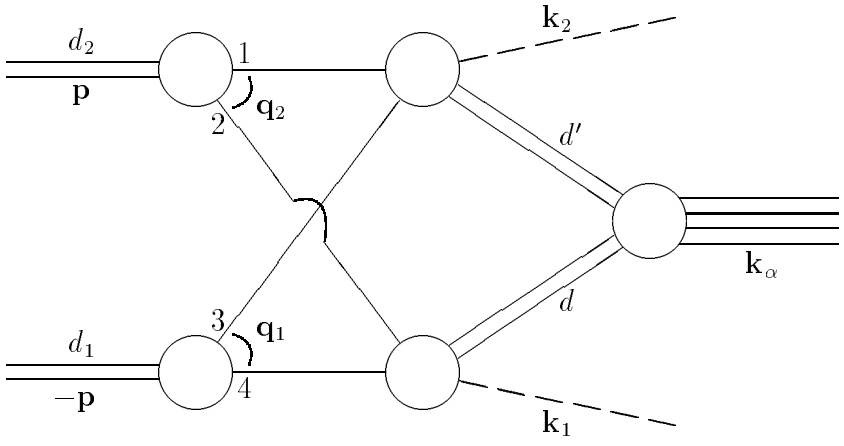

Figure 1: Feynman diagram for the $dd \to \alpha X$ reaction showing the momenta in the overall cm system

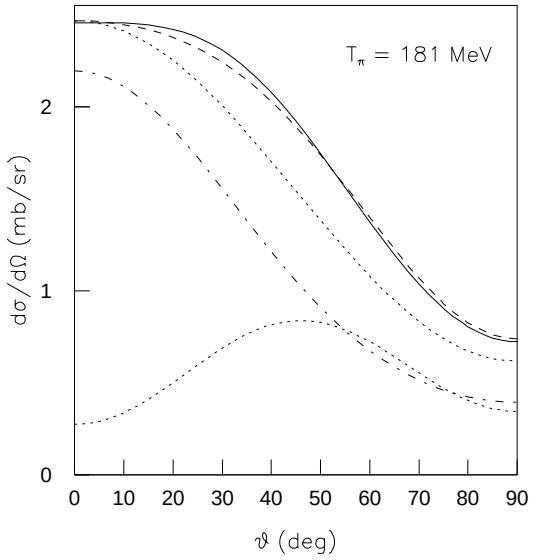

Figure 2: Differential cross section for the $\pi^+ d \to pp$ reaction at $T_\pi = 181$ MeV, calculated with nine amplitudes (dashed line) compared to the differential cross section obtained from the SAID database (solid line). The cross sections for $^1D_2 p$ (uppermost dotted line) and the singlet (dot-dashed line) and triplet (lowest dotted line) amplitudes are also given.

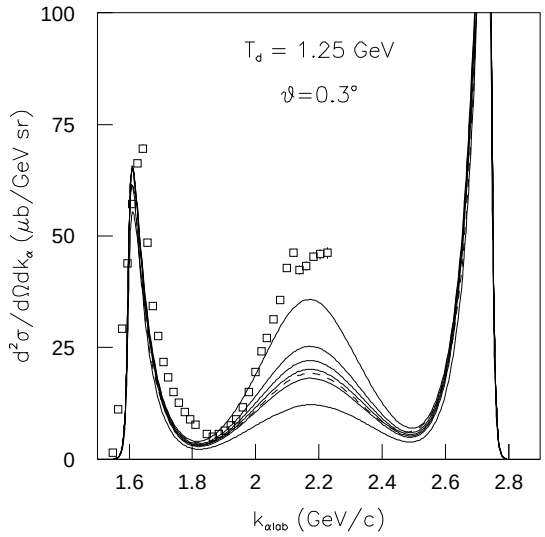

Figure 3: Comparison of cross sections calculated with different α-particle wave functions. Solid lines correspond to the Gaussian wave function with the parameter β (defined in the text) having the values (from bottom to top): 0.55, 0.64, 0.67, 0.70, 0.75, and 1.0 fm^{-1}. For comparison the calculation with the Forest et al. [28] wave function (dashed line), is repeated. The data are from Ref. [6].

T_d (MeV)	787	940	1084	1250	1412	1938
σ_{dd} (mb)	118	122	128	137	145	152
$\frac{1}{2}(\sigma_{pn}+\sigma_{pp})$ (mb)	28	33	36	39	42	44
$\sigma_{\pi\alpha}$ (mb)	100	235	328	332	275	135
$\sigma_{\pi d}$ (mb)	42	96	176	229	185	71
$\mathcal{D}$(estimate)	1.50	1.38	0.77	0.46	0.48	0.78
$\mathcal{D}$(fit)	2.2	0.90	0.72	0.73	0.80	1.0

Table 1: Distortion factor $\mathcal{D}$ calculated according to eq. (3.35) for different dd energies. The total cross section data are from Refs [23, 24, 25, 26]. The estimated reduction factor is compared to the scale factor needed to fit our predictions to data.

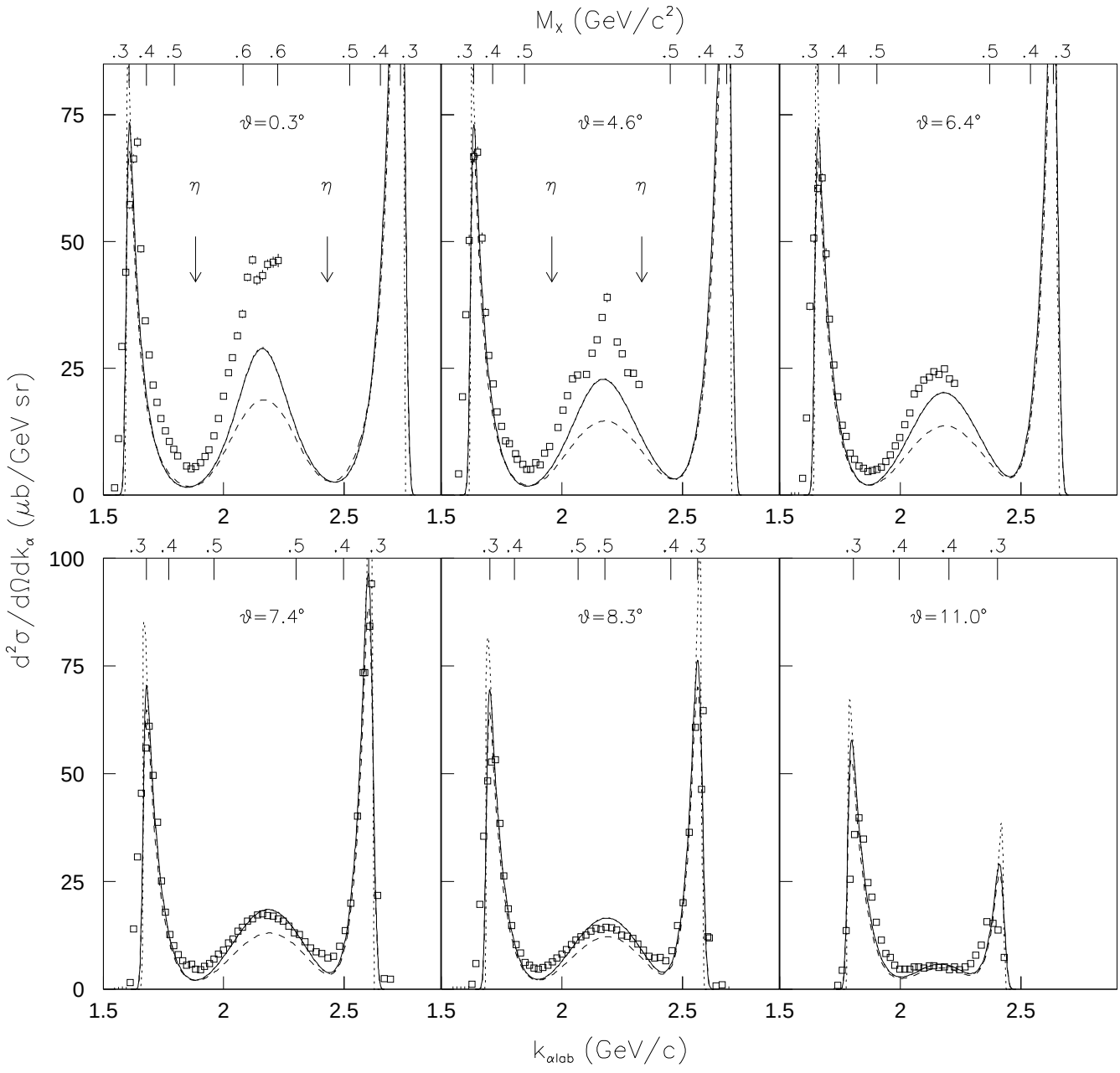

Figure 4: Angular distribution $dd \to \alpha X$ at $T_d = 1.25$ GeV. The smeared E1 (dashed line) and E2 (solid line) calculations are compared to the data of Ref. [6]. For E2 the raw calculations (dotted line) is also given. Our predictions are fitted to the forward (low k_α) ABC peak with a scale factor 0.71, cf. Sec. 3.6.

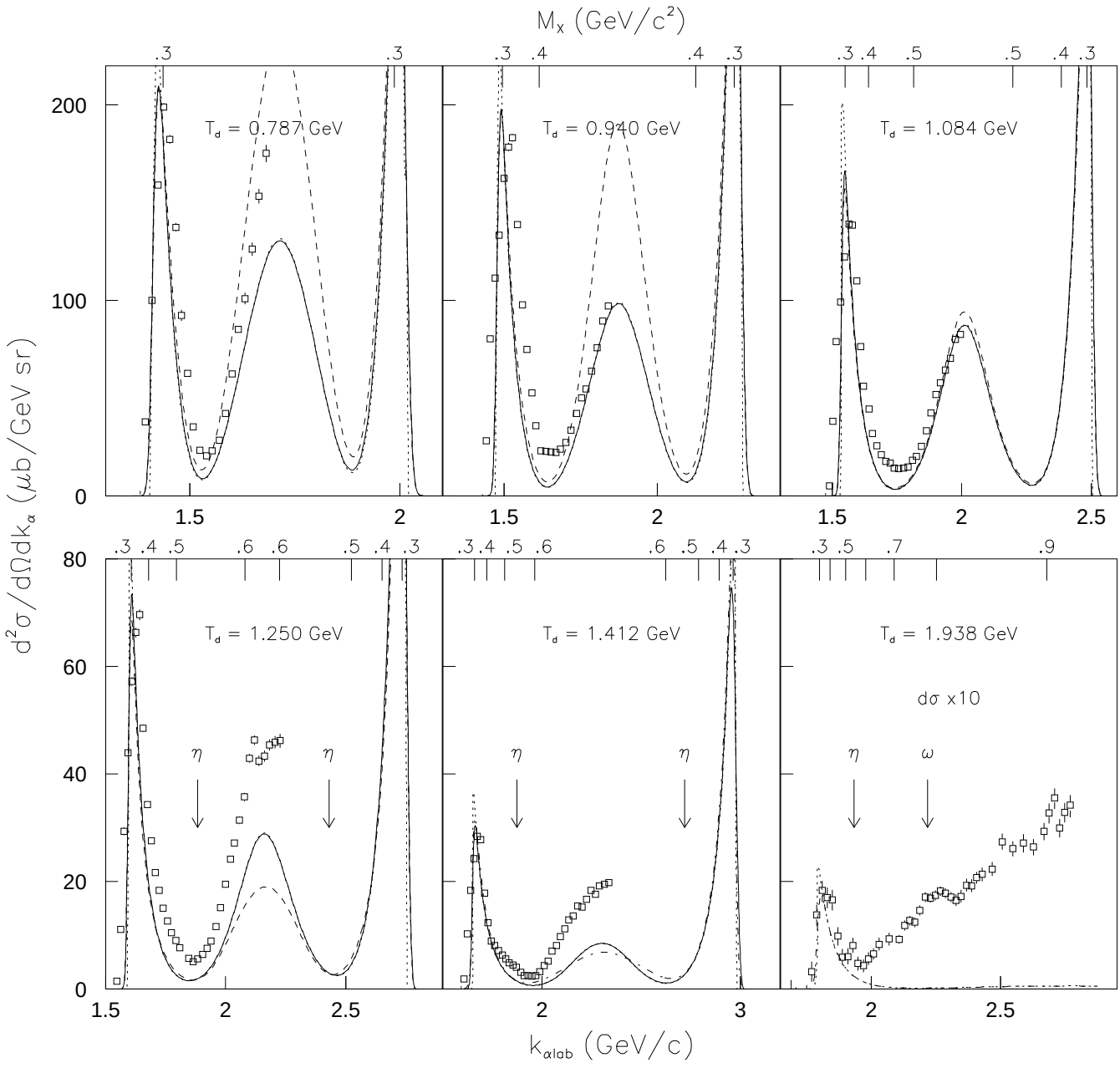

Figure 5: Predictions of the energy dependence of $dd \to \alpha X$ at $\theta_\alpha = 0.3°$ compared to data from Ref. [6]. The different curves are defined as in Fig. 4. Since it is impossible to use E1 at 1.4 GeV, and neither E1 nor E2 at 1.9 GeV, the calculations with constant amplitudes (dot-dashed line) are given at these energies. The calculations are reduced by the scale factors given in Sec. 3.6.

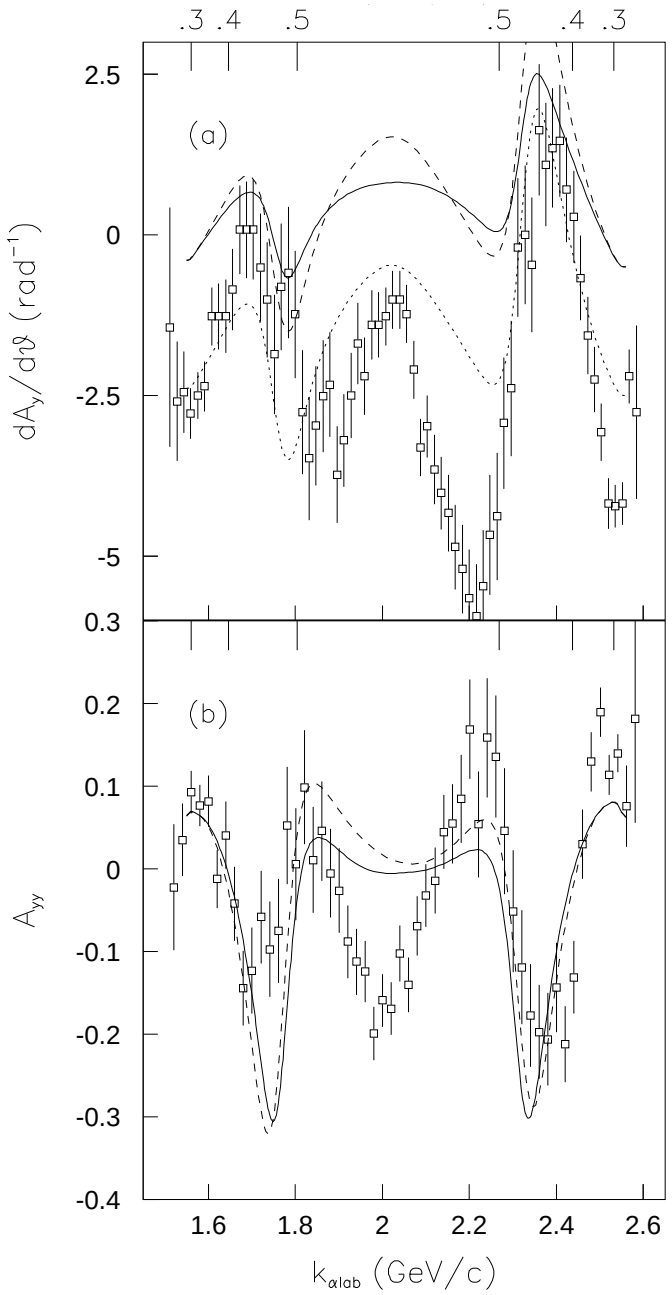

Figure 6: Predictions of forward analyzing powers compared to the SPESIII measurements [7]. Both the E1 (dashed line) and E2 (solid line) calculations are given. The experimental acceptance is incorporated in the theoretical results. **(a)** Average slope of vector analyzing power A'_y. The similarity in shape is more evident after shifting the E1 prediction by -2 rad^{-1} (dotted line). Data are obtained for a range of energies $1.116 < T_d < 1.127$ GeV, while calculations are done at 1.122 GeV. **(b)** Tensor analyzing power A_{yy} at $T_d = 1.116$ GeV.